KJMS 2022 VOL.4 (1): 72-83

KDU Journal of Multidisciplinary Studies (KJMS)

Volume 4. Issue 1 July 2022

DOI: http://doi.org/10.4038/kjms.v4i1.41

USE OF RUBBERIZED CONCRETE TO REDUCE HIGH VELOCITY IMPACT ON WALLS IN TRAINING BASES

P.T.D. Perera[1], and D.D.T.K. Kulathunga[1]

Civil Engineering Department, General Sir John Kotelawala Defense University, Ratmalana, Sri Lanka[1]

ABSTRACT

Discarded waste rubber has become a major problem to the environment due to the increase of rubber usage in the modern world. As a solution, waste rubber can be embedded in rubberized concrete by partially replacing the fine and coarse aggregates. Due to the nature of rubber, there is a high potential for the rubberized concrete to have high impact absorbent properties. Most of the firing rang walls are made with normal concrete and bricks in Sri Lanka. Therefore, this study focuses on investigating the use of rubberized concrete for firing range walls. The study consists of an experimental analysis of live fire tests and a numerical analysis of the high velocity impacts. Penetration depth and crater diameter were taken as the scales of measuring the level of damage to the walls. Numerical analysis results show lower penetration depth in rubberized concrete than in normal concrete. However, experimental analysis shows higher penetration depth in rubberized concrete compared to normal concrete. However, it is worth noticing that the crater diameter and cracks around the penetration are comparatively improved in the case of rubberized concrete. Therefore, rubberized concrete appeared to be a better alternative for firing range walls.

KEYWORDS: *Rubberized Concrete, High Velocity Impacts, Bullet Penetration, Live Fire Test, Experimental Analysis, Numerical Analysis*

Corresponding Author: P.T.D. Perera, Email: *thimira98perera@gmail.com*

1. NTRODUCTION

Disposal of waste rubber causes severe environmental threats specially in developing countries due to the non-biodegradable nature of rubber materials (Edirisinghe, 2013). As a solution for this matter, several tests and studies have been done on rubber granules and crumb rubber to see the possibility of embedding rubber crumbs in concrete as a replacement to aggregates. It was observed through these studies that the rubber crumbs in concrete leads to a considerable drop in the compressive strength. As a result, rubberized concrete was limited only to applications where low level of strength is required. However, it was worth noting that rubber as a material has a high shock absorbent property. Therefore, there is a research interest that arose in analyzing the shock absorbent properties of rubberized concrete.

Military firing ranges are the places where soldiers/ military officers conduct live firing exercises. Current practice is to make firing ranges using brick and concrete walls. However, during the training these walls get damaged and with time the damages become severe. Due to the high shock absorbent properties of rubberized concrete, there is a high potential for rubberized concrete to be a better alternative for the walls in firing ranges. Therefore, this research focuses on studying the feasibility of using rubberized concrete for the walls in firing ranges.

2. LITERATURE REVIEW

Mixing of rubber crumbs to concrete has been found beneficial in different usages such as for lightweight concrete, as a lightweight filler, as a modifier in asphalt paving mixtures and to build crash barriers and bumpers. Most of these applications are owing to the lower density of rubber compared to the conventional aggregates used in concrete. Crumb rubber and chipped rubber are two main forms of rubber waste that can be used as an additive in rubberized concrete. These two forms of rubber are used as an alternative substitute for fine and coarse aggregates, respectively. Previous studies have proven that the fine crumb rubber in concrete gives a better performance than chipped rubber (Gerges, Issa and Fawaz, 2018).

However, many studies have concluded that the rubber aggregates in concrete reduces the compressive strength of concrete drastically with the increase of percentage of rubber in concrete (Gerges, Issa and Fawaz, 2018). This finding demotivated the use of rubberized concrete to a great extent.

However, J. Xue and M. Shinozuka (2013) have shown that the increment in the percentage of crumb rubber additives into the concrete can cause a nonlinear behaviour between stress and strain as shown in Figure 2.1.

According to the previous studies (Senin *et al.*, 2017), the ordinary cement concrete is generally brittle while the addition of crumb rubber in the concrete can increase the impact resistance and ductility.

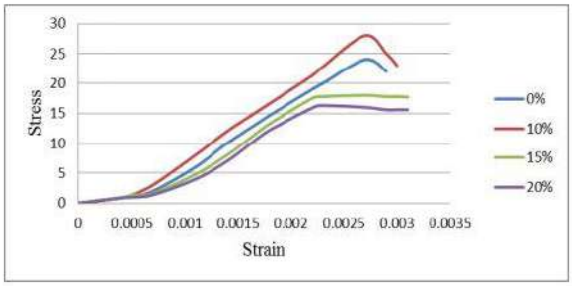

Figure 2.1: Relationship between stress and strain for different crumb rubber percentages in concrete (Dass and Sharma, 2013)

Najim & Hall (2012) has concluded that the bonding between rubber particles and cement paste is weaker compared to the bonding between course aggregate and cement paste, which causes a reduction of compressive strength of rubberized concrete (Najim and Hall, 2012). A study done by Xue and Shonozuka (2013) has also discovered that the compressive strength of rubberized concrete drops due to lack of bonding between rubber and cement particles and they have further discovered that this bond can be improved by adding Silica Fume.

Xue & Shinozuka (2013) have identified that the damping coefficient of rubberized concrete has been amplified compared to normal concrete while a reduction is seen in the seismic response acceleration of the structure. Due to the decrement of the seismic response acceleration of the structure, rubberized concrete is capable of being used as an energy absorption material in order for the reduction in high velocity impacts.

Another study done by Senevirathne et al (2020) has discovered that the impact energy of rubberized concrete increases as the rubber percentage increases (Figure 2.2). They have observed the maximum impact energy when the rubber replacement is 10% of the fine aggregate. (Senevirathne, Kulathunga and Kuruwitaarachchi, 2020)

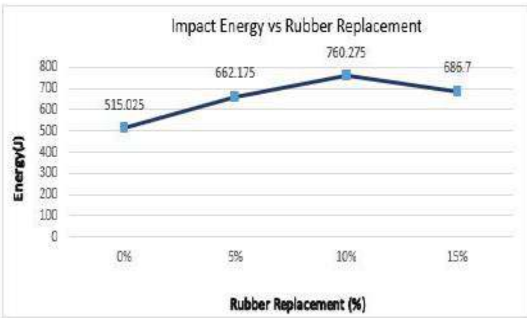

Figure 2.2: Change of Impact Energy (Senevirathne, Kulathunga and Kuruwitaarachchi, 2020)

Concrete can be used as a widely utilized construction material in civil engineering aspects and its impact properties such as crack propagation, penetration depth and perforation are important concerns. The depth of penetration due to high velocity impact has an inverse correlation with the compressive strength (Li, Brouwers and Yu, 2020). The penetration depth of a bullet can be depended on the shape, density, cross-section, pattern of deformation and the kinetic energy of the bullet. A closed cellular structure is developed by the additives in concrete when a bullet impacts on the lightweight concrete (Fabian *et al.*, 1996).

3. METHODOLOGY

This study uses two approaches to reach the conclusions, namely numerical approach and experimental approach.

3.1 Numerical Analysis

For the numerical analysis, LS Dyna software was used. To analyze concrete structures subjected to impacts, the Karagozian & Case Concrete (KCC) model is available in LS-Dyna, and it allows automatic generation of all parameters by importing only the unconfined compressive strength and density of the concrete. Material card (MAT72REL3) which is used for KCC models requires a few parameters to define the material properties of concrete. It includes failure criteria, triaxial strength surface, and strain rate effect. Some parameters such as unconfined compressive strength are automatically generated from the model. Rubberized Concrete material properties are rarely studied by numerical simulations. The material properties for the KCC model should be modified to model the Rubberized Concrete (RubC) accurately differentiating it from Normal Concrete (NC). In this study, the damage to the normal concrete and rubberized concrete caused by a high velocity impact is simulated using the KCC model, and rubberized concrete and normal concrete with compressive strength of 35 MPa were focused in this study

3.1.1 Material Properties

Seconds (s), meters (m), kilograms (kg), and pascals (Pa) are applied as the units for time, mass, length, and stress in the simulation. Parameters needed for the KCC model were extracted from the literature (Gholampour, Ozbakkaloglu and Hassanli, 2017) (Malvar *et al.*, 1997) (Yang *et al.*, 2019)

The values of parameters used for KCC model in this study are listed in Table 3.1 and Table 3.2. In table 3.1 and 3.2, Compression Strength, Tensile Strength, Young's Modulus and Poisson's Ratio are denoted by f_{co}, f_t, E and ν while a_{0m} and a_{0y} represent the maximum and yield cohesion, respectively, and a_{im}, a_{iy} and a_{if} (i = 1, 2) are the hardening parameters performed on the maximum, yield limit and failure, respectively.

Table 3.1: Fitting Results of Normal Concrete (NC) and Rubberized Concrete (RubC) (Gholampour, Ozbakkaloglu and Hassanli, 2017)

Material type	f_{co} (Pa)	a_{om} (pa)	a_{1m}	a_{2m} (Pa^{-1})	a_{0y} (Pa)
NC	34.9e6	1.30e7	0.495	2.4e-9	5.08e6
RubC	32.6e6	1.19e7	0.495	2.63e-9	4.65e6
Material type	a_{1y}	a_{2y} (Pa^{-1})	a_{1f}	a_{2f} (Pa^{-1})	
NC	0.492	1.93e-8	0.754	1.16e-9	
RubC	0.492	2.12e-8	0.754	1.27e-9	

Table 3.2: Static Test Results of Normal Concrete and Rubberized Concrete (NC & RubC) (Yang *et al.*, 2019)

	f_{co} (Pa)	f_t (Pa)	E (Pa)	N
NC	34.9e6	3.06e6	25.85e9	0.21
RubC	32.6e6	3.04e6	24.28e9	0.19

Modified damage parameters of normal and rubberized concrete were also identified from the literature and are listed in the Table 3.3 (Feng *et al.*, 2021)

Table 3.3: Fitted Results of α, αc, αd, and λm (Yang *et al.*, 2019)

Material type	A	α_c	α_d	λ_m
NC	3	0.17	1.92	3.5e-4
RubC	3	0.25	1.55	4.1e-4

According to the test results of Grinys et al. (2013), the fracture energy of the Normal Concrete and Rubberized Concrete were estimated as shown in the Table 3.4.

Table 3.4: Fracture Energy of Normal Concrete and Rubberized Concrete (NC & RubC) (Grinys *et al.*, 2013)

Material Type	Fracture energy Gf (J/m^2)
NC	84.84
RubC	451.57

3.1.2. Equation of State

For the complete characteristics of behaviour of concrete, KCC model required the Equation of State (EOS) which is required to compute the relationship between current pressure and volumetric strain. In the KCC model, EOS#8 (Equation of State, type 8) in LS-DYNA has described the relationship between current pressure (p) and volumetric strain (μ) as the Equation 1 (Livermore Software Technology Corporation (LSTC), 2014)

$$P = C(\mu) + \gamma_0 \theta(\mu) E_0$$

Equation 1: Relationship Between Pressure and Volumetric Strain

Where, E_0 - the internal energy per initial volume

γo - the ratio of specific heat. C(μ) and θ(μ) - the tabulated pressure valuated along a 0K isotherm and tabulated temperature-related parameter as functions of the volumetric strain.

Since the high velocity impact causes damages although it does not have an adequate period for thermal transmission, the temperature-related parameter (θ(μ)) will be neglected in EOS#8.

Table 3.5: EOS parameters of Normal Concrete and Rubberized Concrete (NC & RubC)

Point no.	Volumetric strain	NC		RubC	
		P (C(μ)) (Pa)	K (Pa)	P (C(μ)) (Pa)	K (Pa)
1	0	0	7.44×10^9	0	7.44×10^9
2	-1.5×10^{-3}	1.12×10^7	7.44×10^9	1.12×10^7	7.44×10^9
3	-4.3×10^{-3}	4.92×10^7	1.52×10^{10}	4.75×10^7	1.47×10^{10}
4	-1.01×10^{-2}	7.89×10^7	1.6×10^{10}	7.63×10^7	1.55×10^{10}
5	-3.05×10^{-2}	1.5×10^8	1.9×10^{10}	1.45×10^8	1.84×10^{10}
6	-5.13×10^{-2}	2.26×10^8	2.21×10^{10}	2.19×10^8	2.14×10^{10}
7	-7.26×10^{-2}	3.21×10^8	2.51×10^{10}	3.1×10^8	2.43×10^{10}
8	-9.43×10^{-2}	4.91×10^8	2.74×10^{10}	4.75×10^8	2.65×10^{10}
9	-1.74×10^{-1}	2.87×10^9	6.17×10^{10}	2.77×10^9	5.97×10^{10}
10	-2.08×10^{-1}	4.38×10^9	7.52×10^{10}	4.24×10^9	7.27×10^{10}

The EOS parameters were obtained from previous studies (Feng *et al.*, 2021) and the values are listed in the Table 3.5.

3.1.3 Validation of the KCC model

Single element test was conducted by Yang *et al.*(2019) to validate all the parameters which are required for the KCC model, and it was done by the uniaxial unconfined compression and tension single element test (SET). The tests were conducted to the 1x1x1 cm^3 single element model as shown in the Figure 3.1.

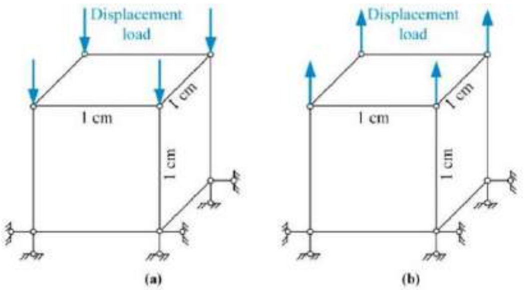

Figure 3.1: Single-element Model for (a) Compression and (b) Tension (Yang *et al.*, 2019)

The results of uniaxial unconfined compression test are shown in the Figures 3.2 and 3.3. It can be seen that the modified KCC model agrees well with the experimental data for rubberized concrete as well as for normal concrete.

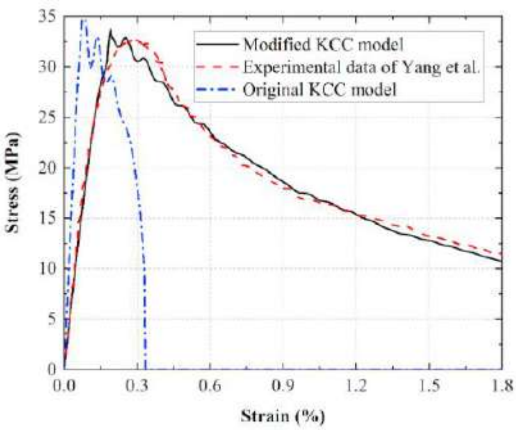

Figure 3.2: Compressive Stress-strain Curve of Rubberized Concrete (Yang *et al.*, 2019)

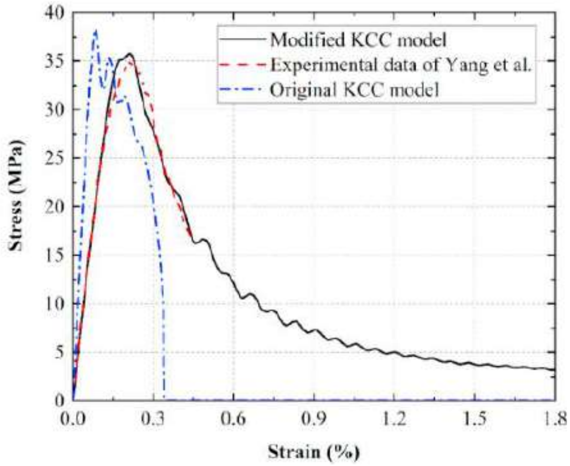

Figure 3.3: Compressive Stress-strain Curve of Normal Concrete (Yang *et al.*, 2019)

The modified KCC model tensile stress strain curve overlaps with the empirical formula in Figure 3.4, indicating that it is more relatable than the original KCC model tensile stress strain curve.

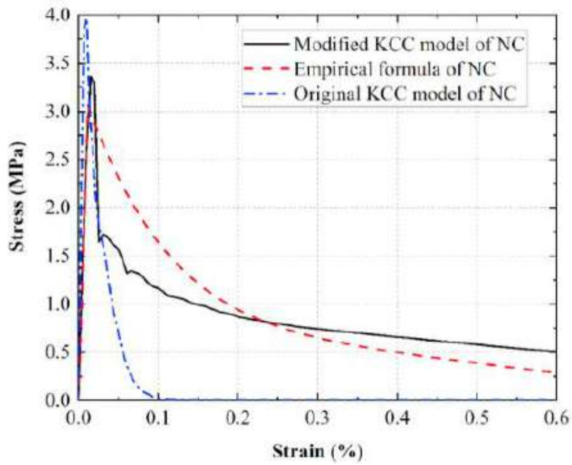

Figure 3.4: Comparison Between Modified KCC Model, Original KCC Model, and Empirical Formula of Normal Concrete (Yang et al., 2019)

3.1.4 Projectile Material Properties

Since the steel core of a projectile (bullet) has the maximum mass and volume compared to other components, namely copper-plated steel jacket and lead filler, steel was considered as the material of the projectile. In the LS-Dyna simulation, the

*MAT_ JOHNSON_COOK material was used to simulate the projectile. The material properties which were used for the projectile are listed in Table 3.6 (Carbajal, Jovicic and Kuhlmann, 2011).

Table 3.6: Johnson - Cook Material Model Properties (Carbajal, Jovicic and Kuhlmann, 2011)

Bullet Component	7.62x39mm mild steel core
Density (ρ) (kg/m^3)	9765.4
Shear modulus (G) (Pa)	1.22×10^{10}
Young's Modulus (E) (Pa)	3.172×10^{10}
Poisson’s Ratio	0.3
A (Pa)	2.344×10^{8}
B (Pa)	413.8×10^{8}
N	0.25
C	0.00333
M	1.03
D_1	5.625
D_2	0.3
D_3	-7.2
D_4	-0.0123
D_5	0

3.1.5 Numerical Simulation

In the numerical simulation, the projectile was shot into normal concrete which has the strength of 35MPa and rubberized concrete which has the strength of 32.6MPa concrete targets.

To reduce the run time, only a quarter of the concrete block and projectile was modelled as shown in the Figures 3.5 and 3.6, and the projectile was initiated near the concrete target. The concrete block was fixed in three directions and throughout the simulation, the concrete block and the projectile were fixed on symmetric planes.

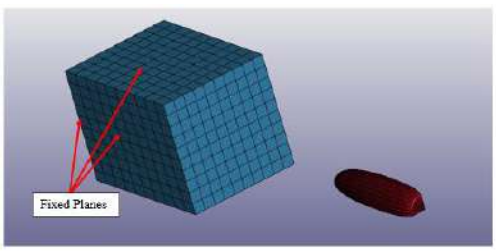

Figure 3.5: Numerical Simulation; Fixed Planes

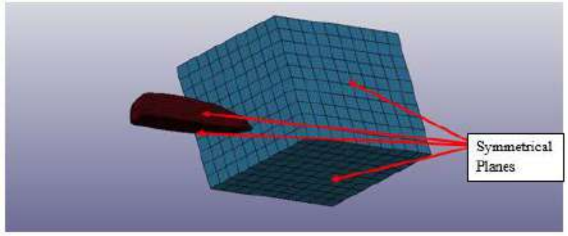

Figure 3.6: Numerical Simulation; Symmetrical Planes

Elements in the fixed planes are restricted in 3 directions while the elements in the symmetrical plane are allowed to move along the plane. Both the concrete block and projectile are made with solid elements. Therefore, the contact between projectile and concrete surface had to be defined through erosion criteria. *MAT_ADD_ EROSION in LS-Dyna is used to define the maximum principal strain since KCC model has no obtainable element erosion criteria. Since the projectile has a high velocity, the termination of the simulation was done with seconds (s).

3.2 Experimental Analysis

3.2.1 Preparation of Samples

Firstly, the sieve analysis was done to compare the particle size distribution of varying fine aggregate types (river sand and crumb rubber) with the lower and upper bounds of BS882 – specification for aggregates from natural sources for concrete.

To increase the bond between crumb rubber and concrete components, crumb rubber needs surface modification which helps to improve the crumb rubber to absorb some amount of water. Before using the crumb rubber in concrete, the surface modification was done by soaking rubber particles in 1N solution of NaOH (Sodium Hydroxide) for about 1 and ½ hours. The crumb rubber particles were settled after 1 and ½ hours. After it soaked well, the rubber particles were washed with clean water to reduce the basicity.

3.2.2 Concrete Mix Design

The mixed design was done according to the British Standards (BS). The grade of Normal Concrete was taken as M25 (25 N/mm^2). The fine aggregate for the Rubberized Concrete was replaced by 10% of sand with crumb rubber.

Table 3.7: Mix Proportions of Normal Concrete and Rubberized Concrete (NC & RubC)

Quantities	Crumb Rubber (kg)	Cement (kg)	Water (kg)	Fine aggregate (kg)	Coarse aggregate (kg) / 10mm
Per m3 (to nearest 5kg) for NC	-	375	205	805	985
Per m3 (to nearest 5kg) for RubC	80	375	205	725	985

According to the range design criteria ('RANGE DESIGN CRITERIA Office of Health , Safety and Security', 2012), the thickness of material to stop the penetration of 7.62mm caliber, 7in (=177.8mm) minimum thickness is required for the concrete material. Therefore, the thickness for the samples of concrete blocks is selected as 200mm. The dimension of each sample concrete block is 250x250x200mm.

3.2.3 Live Fire Test

Live fire test was carried out by using 4 samples of Normal Concrete Blocks (NC1, NC2, NC3 & NC4), 4 samples of Rubberized Concrete (RC1, RC2, RC3 & RC4) and 2 samples of Masonry Blocks (MB1 & MB2).

Attention was paid to the following points while conducting the Live-fire tests:

- It is necessary to determine the depth of penetration for single strikes at a single spot on the bullet trapping block.
- Target should be maintained in such a way that the spalling of concrete is avoided

Live-fire testing was done at an outdoor range. The shooter to target distance was maintained at 13m**.** The test blocks were placed in a steel frame which can handle the sudden impacts and the steel frame was levelled from the split-level and grounded as shown in the Figure 3.7.

Figure 3.7: Steel Frame

The rifle was mounted and maintained the level on a steel frame. The experimental setup is shown in the Figure 3.8.

Figure 3.8: Experimental Setup

Damages on the concrete due to a bullet can occur in 4 methods. They are Ricochet, Perforate, Penetration and Fragmentation. In this experiment, the bullets were trapped inside the blocks due to Penetration. After each concrete block was shot, the bullets were safely removed with a tweezer. Before extracting the bullet, the penetration path was drilled and expanded to remove the bullet. There are 3 types of bullet deformations. They are Deform, Full Fragment and Partial Fragment. After all the bullets were removed, it was seen that the bullets were deformed by Partial Fragments.

The apparent depth of penetration and the crater of the bullet hole were measured using a vernier caliper. The craters of the bullet holes were measured by taking the average diameter of the crater.

4. RESULTS

4.1 Numerical Analysis

The penetration depth of the concrete was measured under four different projectile velocities: 200ms^{-1}, 300ms^{-1}, 400ms^{-1} and 500ms^{-1}. Figure 4.1 and 4.2 show the deformed shapes of the normal concrete and rubberized concrete models after the impact of 300ms^{-1} projectile velocity.

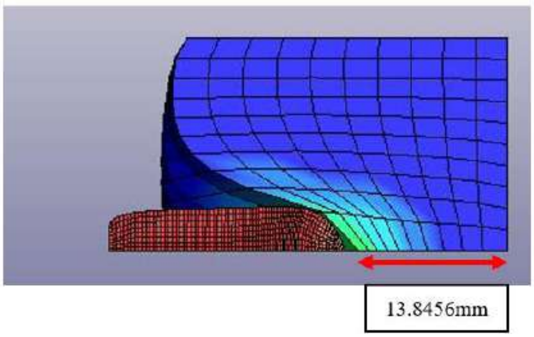

Figure 4.1: Normal Concrete Deformed Shape of the Model after the Impact under 300ms^{-1} Projectile Velocity

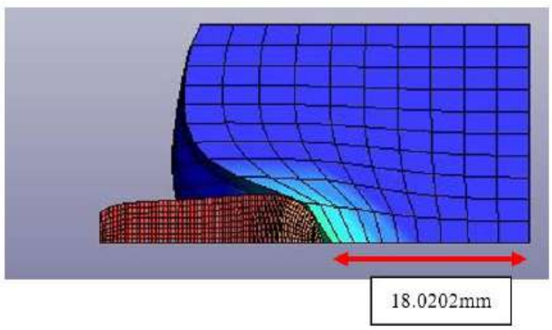

Figure 4.2: Rubberized Concrete Deformed Shape of the Model after the Impact under 300ms^{-1} Projectile Velocity

Velocity of the projectile versus penetration depth is shown in Figure 4.3 for normal concrete and rubberized concrete.

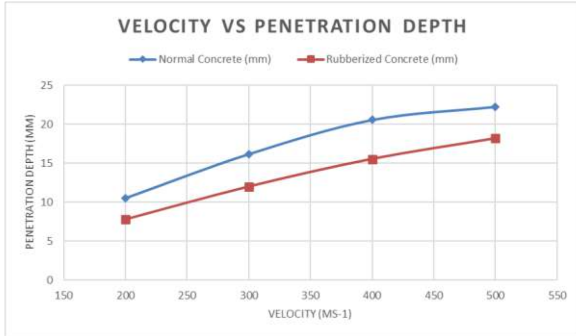

Figure 4.3: Velocity vs Penetration Depth

4.2 Experimental Analysis

4.2.1 Preparation of Samples

Figure 4.4 shows that the river sand and the mix of river sand and crumb rubber, which are used to make normal concrete and rubberized concrete respectively were within the upper and lower bounds of the BS882 requirement of concrete.

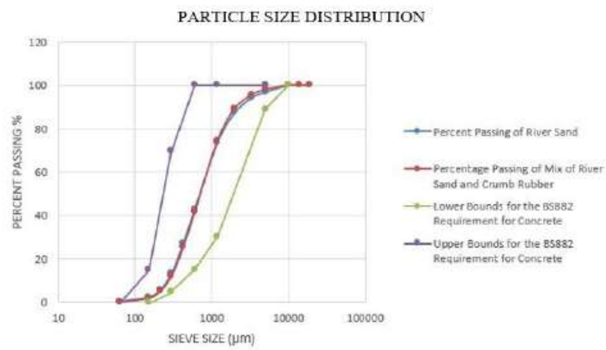

Figure 4.4: Particle Size Distribution

The specific gravity of the sand sample is 1.56Mg/m^3 while the specific gravity of the crumb rubber sample is 0.97Mg/m^3, which makes the specific gravity of the mixed ($Gmixed$) sample (the sand mixed with 10% of crumb rubber) to be 1.47Mg/m^3. The mix of sand and crumb rubber has a lower specific gravity compared to the specific gravity of the sand. Therefore, the crumb rubber reduces the specific gravity of the sand. The partial replacement of fine aggregate by 10% from crumb rubber results in the slump value getting decreased. Slump values are shown in Table 4.1.

Table 4.1: Slump Values of Normal Concrete and Rubberized Concrete (NC & RubC)

Sample	Slump Values (mm)
NC	100
RubC	90

4.2.2 Compressive Strength Test Results

The compressive strength of concrete was measured after 56 days of curing. Table 4.2 shows the compressive strength values of each test samples.

Table 4.2: Compressive Strength Test Results

Mixture	Weight (kg)	Density (kg/m^3)	Compressive strength (N/mm^2)	Compressive strength decrease (%)
Control mix				
1) Sample 1	7.846	2324.74	34.290	
2) Sample 2	7.871	2332.15	36.025	
Average	7.8585	2328.445	35.1575	-
10% Rubber Replacement				
1) Sample 1	6.336	1877.33	7.084	
2) Sample 2	6.088	1803.85	6.627	
Average	6.212	1840.59	6.8555	80.5%

4.2.3 Live Fire Test Results

Figure 4.5, Figure 4.6 and Figure 4.7 show the damages occurred in 3 samples of Normal Concrete (NC1), Rubberized Concrete (RC1), and Masonry Blocks (MB2) respectively.

Figure 4.5: Damage Pattern on the NC1 Block

Figure 4.6: Damage Pattern on the RC1 Block

Figure 4.7: Damage Pattern on the MB2 Block

Penetration depths obtained for each sample are shown in Figure 4.8.

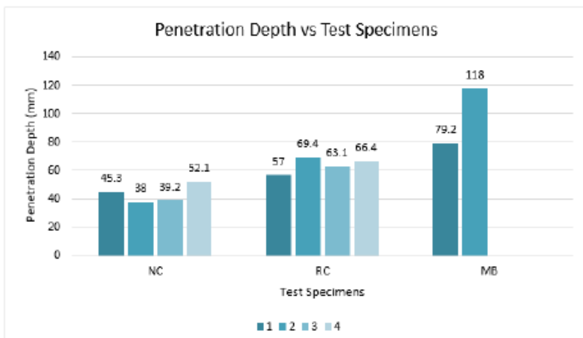

Figure 4.8: Penetration Depth vs Test Specimens

Crater diameter values obtained for each test specimens are shown in the Figure 4.9.

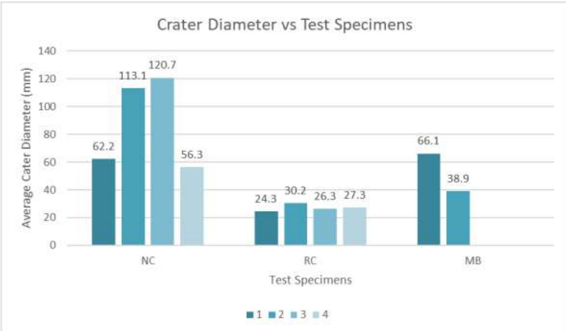

Figure 4.9: Crater Diameter vs Test Specimens

5. DISCUSSION

5.1 Numerical Analysis

According to the results obtained for the numerical analysis, it was seen that the penetration depth of rubberized concrete is lesser than the penetration depth of normal concrete for all the projectile velocities (200ms^{-1}, 300ms^{-1}, 400ms^{-1} and 500ms^{-1}) considered in the analysis (Figure 4.3). Also, it was noticed that the penetration depth increases as the velocity of the projectile increases.

5.2 Experimental Analysis

It was clear from the results shown in Figure 4.4 that the sieve analysis results of the mix of river sand and crumb rubber are acceptable as per the requirements specified in BS882.

As per the compressive strength results obtained for the rubberized concrete (Table 4.2), it can be seen that there is a significant drop in compressive strength of rubberized concrete. Although, it was evident from the literature also that the compressive strength significantly drops with the addition of rubber, the drop obtained in this study is comparably higher.

Figure 4.5, Figure 4.6 and Figure 4.7 show the damage patterns for each type of test specimens and Figure 4.8 shows the penetration depths. The average penetration depth of the bullet into the normal concrete Block is 43.65mm (penetration as a percentage is 21.83%).

The average penetration depth of the bullet into the Rubberized Concrete Block is 63.9mm (penetration as a percentage is 31.95 %). In the case of masonry walls, only one sample could be used to measure the penetration depth and crater diameter as the other samples were damaged severely due to the impact. The penetration depth of the bullet into the masonry block is 118mm (penetration as a percentage is 59%). Therefore, in the experimental analysis, penetration depths of the Rubberized Concrete blocks were observed to be higher than that of the normal concrete blocks but less than that of masonry blocks. This contradicts the results observed in the numerical analysis. However, it should be noted that in the case of the numerical analysis, the strengths used for normal and rubberized concrete were approximately the same. In the case of experimental analysis, the strength of rubberized concrete drastically reduced due to the addition of rubber. Therefore, in the experimental analysis, the rubberized concrete samples are significantly lower in strength than the normal concrete sample. This reduction in strength caused rubberized concrete to show a higher penetration depth during the experimental analysis. If the numerical analysis was conducted as per the strengths achieved in the experimental analysis, the results could have been compared effectively and stronger conclusions could have been drawn. However, due to the unavailability of material properties to fit the KCC model, it was not possible to conduct the numerical analysis for the strengths achieved in the experimental analysis.

Figure 4.9 shows the crater diameter for each specimen. The average crater diameter of normal concrete, rubberized concrete and masonry blocks were 88.1 mm, 27 mm and 38.9 mm, respectively. It was clear from the results that the crater diameter and the visible cracks of the Rubberized Concrete blocks were less than those of the normal concrete blocks and the masonry blocks. The failure pattern observed in the samples shows that rubberized concrete targets are less damaged compared to the normal concrete and masonry samples despite the lower strength of the rubberized concrete. Therefore, it is evident from the results that rubberized concrete has a potential as a better alternative to firing range walls.

6. CONCLUSIONS

This study uses both the numerical and experimental approaches to investigate the potential of Rubberized Concrete to be used in firing range walls. Live firing test was done in the experimental analysis. The damage was identified by the penetration depth of the projectile. The numerical analysis was carried out using LS-DYNA software.

For the numerical analysis, the strength of the normal and rubberized concrete samples was considered as 35 MPa. This strength was selected due to the availability of material properties for the KCC model in the literature. Results of numerical analysis show that rubberized concrete has a lower penetration depth compared to normal concrete, which implied that rubberized concrete has a higher shock absorbing property.

The experimental analysis was done for normal concrete samples of 25 MPa. The strength of the rubberized concrete samples used in the experiment is found to be considerably lower than the strength of normal concrete. Therefore, in the experiment results, the rubberized concrete samples showed a higher penetration depth than the normal concrete. However, the damage occurred is considerably lower in rubberized concrete samples despite the lower strength. Therefore, rubberized concrete seems to be a better solution in the case of resisting the impact, and hence it appeared to be a better alternative for the walls in firing ranges. Therefore, it is worth investing further effort in a detailed analysis to identify the feasibility of rubberized concrete in applications such as walls in firing ranges.

7. REFERENCES

Carbajal, L., Jovicic, J. and Kuhlmann, H. (2011) ‘Assault riffle bullet-experimental characterization and computer (FE) modeling’, *Conference Proceedings of the Society for Experimental Mechanics Series*, 6, pp. 647–664. doi: 10.1007/978-1-4614-0222-0_77.

Edirisinghe, J. C. (2013) ‘Community Pressure and Environmental Compliance : Case of Rubber Processing in Sri Lanka’, pp. 14–23.

Fabian, G. L. *et al.* (1996) ‘Use of Shock-Absorbing Concrete [SACON] as an Environmentally Compatible Bullet-Trapping Medium on Small-Arms Training Ranges’, *Proceedings of the Tri-Service Environmental Technology Workshop, ‘Enhancing Readiness Through Environmental Quality Technology’ Held in Hershey, PA on 20-22 May 1996*.

Feng, W. *et al.* (2021) ‘Numerical study on blast responses of rubberized concrete slabs using the Karagozian and Case concrete model’, *Journal of Building Engineering*, 33(May 2020), p. 101610. doi: 10.1016/j.jobe.2020.101610.

Gerges, N. N., Issa, C. A. and Fawaz, S. A. (2018) ‘Rubber concrete: Mechanical and dynamical properties’, *Case Studies in Construction Materials*, 9, p. e00184. doi: 10.1016/j.cscm.2018.e00184.

Gholampour, A., Ozbakkaloglu, T. and Hassanli, R. (2017) ‘Behavior of rubberized concrete under active confinement’, *Construction and Building Materials*, 138, pp. 372–382. doi: 10.1016/j.conbuildmat.2017.01.105.

Grinys, A. *et al.* (2013) ‘Fracture of concrete containing crumb rubber’, *Journal of Civil Engineering and Management*, 19(3), pp. 447–455. doi: 10.3846/13923730.2013.782335.

Koksal, A. (2002) ‘Specification for aggregates from natural sources for concrete’, (December).

Kong, X. *et al.* (2017) 'Modified K&C model for cratering and scabbing of concrete slabs under projectile impact', *International Journal of Impact Engineering*, 108, pp. 217–228. doi: 10.1016/j.ijimpeng.2017.02.016.

Li, P. P., Brouwers, H. J. H. and Yu, Q. (2020) 'Influence of key design parameters of ultra-high performance fibre reinforced concrete on in-service bullet resistance', *International Journal of Impact Engineering*. doi: 10.1016/j.ijimpeng.2019.103434.

Livermore Software Technology Corporation (LSTC) (2014) *Keyword User ' S Manual Volume 1*.

Malvar, L. J. *et al.* (1997) 'A plasticity concrete material model for DYNA3D', *International Journal of Impact Engineering*, 19(9–10), pp. 847–873. doi: 10.1016/s0734-743x(97)00023-7.

Najim, K. B. and Hall, M. R. (2012) 'Mechanical and dynamic properties of self-compacting crumb rubber modified concrete', *Construction and Building Materials*, 27(1), pp. 521–530. doi: 10.1016/j.conbuildmat.2011.07.013.

'RANGE DESIGN CRITERIA Office of Health , Safety and Security' (2012).

Senin, M. S. *et al.* (2017) 'A review on the suitability of rubberized concrete for concrete bridge decks', *IOP Conference Series: Materials Science and Engineering*, 271(1). doi: 10.1088/1757-899X/271/1/012074.

Xue, J. and Shinozuka, M. (2013) 'Rubberized concrete: A green structural material with enhanced energy-dissipation capability', *Construction and Building Materials*. doi: 10.1016/j.conbuildmat.2013.01.005.

Yang, F. *et al.* (2019) 'Experimental and numerical study of rubber concrete slabs with steel reinforcement under close-in blast loading', *Construction and Building Materials*, 198, pp. 423–436. doi: 10.1016/j.conbuildmat.2018.11.248.

Koksal, A. (2002) 'Specification for aggregates from natural sources for concrete', (December).